Marine and Petroleum Geology 170 (2024) 107130

Contents lists available at ScienceDirect

Marine and Petroleum Geology

journal homepage: www.elsevier.com/locate/marpetgeo

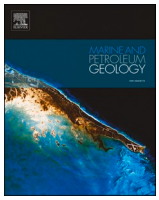

The influence of shallow-water methane emissions on foraminiferal assemblages: The case of Scoglio d'Affrica (Northern Tyrrhenian Sea, Mediterranean Sea)

Letizia Di Bella [a,*], Martina Pierdomenico [b], Aida Maria Conte [b], Irene Cornacchia [b], Tania Ruspandini [a], Daniele Spatola [a], Stanley Eugene Beaubien [a], Sabina Bigi [a], Alessia Conti [b], Giovanni Gaglianone [a], Michela Ingrassia [b], Francesco Latino Chiocci [a,b], Daniele Casalbore [a,b]

[a] Department of Earth Sciences, Sapienza University, Piazzale Aldo Moro 5, Rome, Italy
[b] Research Council of Italy, Institute of Environmental Geology and Geoengineering (CNR-IGAG), UOS, Department of Earth Sciences, Sapienza University, Piazzale Aldo Moro 5, Rome, Italy

ARTICLE INFO

Keywords:
Benthic foraminifera
Extreme environment
Methane emissions
Mud volcano
Tuscan archipelago

ABSTRACT

Microfaunal analyses were conducted near Scoglio d'Affrica in the Tuscan Archipelago (Northern Tyrrhenian Sea), to study the response of benthic foraminifera to methane (CH_4) venting activity that occurs in this shallow water environment. Our data show that sedimentary processes linked to the CH_4 emissions exert a strong influence on foraminiferal assemblages, resulting in a very patchy spatial distribution linked to complex abiotic and biotic interactions. Methane emissions and mud represent the two main stressor factors for the benthic foraminiferal assemblages, although at present it is not possible to determine which impact dominates.

Five different morphological settings, controlled by venting activity, were defined on and off the mud volcanoes (MVs). Each of these settings has distinct assemblages: 1) areas with strong emission activity at the top of the MVs, locally associated with gryphons and mudflows, where the environmental conditions are clearly prohibitive for foraminiferal life; 2) mud flows along the MV flanks, where overlapping mudflows likely limit foraminiferal colonization; 3) muddy sediments associated with weak emissions where the development of foraminiferal community is favored, although with differences in terms of density, diversity and compositional features linked to the timing of colonization by each species; 4) intermatte zones with scarce or absent emissions, characterized by typical shallow water taxa indicative of well-oxygenated and highly hydrodynamic conditions; and 5) *Posidonia oceanica* substrates, characterized by higher foraminiferal content on the leaves compared to the rhizomes and surrounding sediments; indeed, sediments and rhizomes were more impacted by emissions, whereas *Posidonia* leaves offer "refugia" and a more mitigated environment.

Although it is difficult to define a pattern of biota response and to identify seep-exclusive taxa, foraminifera can represent good environmental proxies for both monitoring the variability of recent venting activity and detecting stressed conditions occurring in the geological record. The seafloor around Scoglio d'Affrica represents a very promising study site for multidisciplinary marine research regarding venting activity, geochemistry of cold seep fluids and their effects on benthic organisms.

1. Introduction

Methane (CH_4) is an important greenhouse gas, with a global warming potential about 20 times larger than carbon dioxide (CO_2) on a 100-year horizon (Ramaswamy et al., 2001). In the marine environment, coastal areas represent methane hotspots, releasing around 8 to 13 Tg CH_4 yr^{-1} (Bange et al., 1994; Schorn et al., 2022; Rosentreter et al., 2021) and greatly exceeding emissions from the open ocean

* Corresponding author.
E-mail addresses: letizia.dibella@uniroma1.it (L. Di Bella), martina.pierdomenico@cnr.it (M. Pierdomenico), aidamaria.conte@cnr.it (A.M. Conte), irene.cornacchia@igg.cnr.it (I. Cornacchia), tania.ruspandini@uniroma1.it (T. Ruspandini), daniele.spatola@uniroma1.it (D. Spatola), stanley.beaubien@uniroma1.it (S.E. Beaubien), alessia.conti@cnr.it (A. Conti), gaglianone.giovanni@uniroma1.it (G. Gaglianone), michela.ingrassia@cnr.it (M. Ingrassia), francesco.chiocci@uniroma1.it (F.L. Chiocci), daniele.casalbore@uniroma1.it (D. Casalbore).

https://doi.org/10.1016/j.marpetgeo.2024.107130
Received 1 May 2024; Received in revised form 19 September 2024; Accepted 23 September 2024
Available online 26 September 2024

(0.6–1.2 Tg CH_4 yr^{-1}, Rhee et al., 2009). Seafloor areas affected by methane emissions are known as cold seeps, which can be associated with the development of morphologically negative and/or positive structures, such as pockmarks and mud volcanoes (e.g., Hovland et al., 2002; Kopf et al., 2002; Mazzini et al., 2017). Both these structures are the shallow expression of deep fluid migration along fault dislocations and other structural features (Judd and Hovland, 2009). These seafloor areas represent a very peculiar and extreme environment that is considered as a hotspot for most associated benthic assemblages (e.g., Ingrassia et al., 2015; Di Bella et al., 2016; Di Bella et al., 2022). On the other hand, the occurrence of violent gas outbursts or mudflows from active mud volcanoes may represent catastrophic event for benthic micro- and macro communities (Jerosch et al., 2007). Methane emissions from aquatic ecosystems are not well constrained due to the lack of observations and numerous uncertainties regarding the functioning of the associated ecosystems. The complexity of the interaction between different ecological factors characterizing the shallow fluid emissions makes it difficult to assess the pattern of biota responses in *situ*. Literature data have demonstrated the value of foraminifera as proxies for environmental characterization and for detecting contamination of seafloor ecosystems by methane (Dando et al., 1991; Gupta et al., 1997; Rathburn et al., 2000; Panieri, 2003; Portnova et al., 2014; Schwing et al., 2015; Yanko et al., 1999, 2017, 2023; Shnyukov and Yanko-Hombach, 2020). However, the influence of methane seepage on organisms is still poorly understood.

For example, published data have shown that it can have a positive, negative or null impact on meiobenthos (Dando and Hovland, 1992; Jensen et al., 1992; Polikarpov et al., 1998). However, little is known about its precise impact on infaunal and epifaunal living organisms. It is not clear if biogenic (Denman et al., 2007; Conrad, 2009; Schorn et al., 2022) or thermogenic (Meister et al., 2018) methane affect the microfaunal taxonomic and spatial distribution. Some researchers report a positive effect of methane on meio-benthic organisms, especially if they live directly on methane seeps (Luth et al., 1999; Rathburn et al., 2003; Wiedicke and Weiss, 2006; Panieri, 2006; Cook et al., 2011) where the development of microbial materials represents a further source of food for foraminifera. Similar results were observed from the fossil record in the Pacific Ocean during the Paleocene-Eocene Thermal Maximum (Thomas, 2003). Opposite findings were found at both shallow- and deep-water sites, where stressing conditions for the foraminiferal assemblages resulted in a decrease in faunal density and loss of biodiversity. In these environmental settings, the foraminiferal assemblages are always dominated by opportunistic species (Panieri, 2003; Pletnev et al., 2014). Likewise, a recent study in the Northwestern part of the Black Sea (Yanko et al., 2023) reached the same conclusions, showing lower simple diversity and abundance as well as smaller sizes of foraminiferal tests compared to those from areas not affected by hydrocarbon emissions, indicating that reproduction and growth strongly inhibited.

Other studies suggest that the occurrence of characteristic species or a specific composition of benthic foraminiferal assemblages may indicate methane release at the seafloor (e.g., Mackensen et al., 2006; Bernhard et al., 2009). This observation could be of great interest for paleoenvironmental reconstruction of the fossil record to investigate the relationship between methane and climate. For example, the release of methane from large marine reservoirs has been linked to climate change, both as a causal mechanism and as a consequence of temperature changes, during the Paleocene and Quaternary period (Rathburn et al., 2000; Panieri et al., 2014). One way to reconstruct past marine methane emissions is by carbon isotope ($\delta^{13}C$) analysis of benthic tests (e.g., Kennett et al., 2000; Panieri et al., 2016). Generally, depleted $\delta^{13}C$ values differentiate environments with methane venting activity from those that are not affected (Rathburn et al., 2003; Hill et al., 2004; Panieri et al., 2014). However, differences can also be caused by deep versus shallow environments and on the basis of local microhabitats. For example, the positive $\delta^{13}C$ signature of epifaunal taxa is due to the buffer effect of photosynthesis activity, while in infaunal species the signature results are more depleted. Even if this strengthens the relationship between environmental conditions and ecological preferences of the different species (McCorkle et al., 1990, 1997; Rathburn et al., 1996, 2000), it shows the importance of a conservative approach when using this type of analysis.

In this work we report a study on benthic foraminiferal assemblages associated with active methane seepage offshore the Scoglio D'Affrica islet, along the Elba-Pianosa ridge in the northern Tyrrhenian Sea (western Mediterranean). On March 16th, 2017, a violent gas eruption occurred in this area, with the emission of a "dirty water" column rising up to 10 m above the sea level from a shallow-water mud volcano (Casalbore et al., 2020). So far, marine studies related to Scoglio d'Affrica have focused on the characterization of geomorphological (Motteran and Ventura, 2005; Spatola et al., 2023), geochemical (Meister et al., 2018; Saroni et al., 2020) and microbial (Ruff et al., 2016; Schorn et al., 2022) processes, while there is no information about the microfauna.

The aims of the present research are: 1) to determine the species composition of the benthic foraminiferal assemblages associated with shallow-water fluid emissions; 2) to assess the effect of fluid emissions on different microhabitats considering epiphytic, epifaunal and infaunal foraminifera; 3) to investigate the effect of methane on biomineralization processes; and 4) to provide new constraints on the ecological behavior of foraminiferal species in response to extreme conditions caused by methane release. These objectives aim to increase the knowledge on the microfaunal response in this extreme environment as a proxy to improve reconstructions of methane release in the past and better predict the impact of future climate warming on methane seepage.

2. Geological setting

The Scoglio d'Affrica islet lies in the southernmost part of the Elba-Pianosa ridge (northern Tyrrhenian Sea), a mainly submarine, north-south elongated morpho-structural high separating the Tuscany Shelf to the east from the Corsica Basin to the west (Fig. 1). The geological evolution of this area was related to the opening of the northern Tyrrhenian Sea due to the eastward rollback of the west-dipping Adria-Paleo-European subduction system (e.g., Carminati and Doglioni, 2012). Shallow marine Pleistocene calcarenites outcrop on Scoglio D'Affrica islet, lying above Triassic-Lower Jurassic limestones and the metamorphic basement (Cornamusini et al., 2002; Motteran and Ventura, 2005). The surrounding area was investigated by the oil and gas company AGIP in the 1970s through high-penetration seismic profiles and explorative work identified a thick succession of Eocene–Oligocene siliciclastic deposits together with gas pockets located at different stratigraphic levels within the turbiditic succession (Cornamusini and Pascucci, 2014). Widespread seafloor seepage has been reported by scuba divers since the 1960s, with a total gas flux rate estimated to be around 700 m^3/day for the entire area (Del Bono and Giammarino, 1968; Barletta et al., 1969). According to these authors, the main gas was CH_4 (around 80%), with minor percentages of N_2, O_2, and CO_2. Recent gas sampling from active mud volcanoes identified in the study area also reported methane as the dominant gas component (approximately 96% of the total volume) and minor gases represented by carbon dioxide, nitrogen, ethane, and helium (Saroni et al., 2020). Based on $\delta^{13}C$-CO_2 and $\delta^{13}C$-CH_4 isotopic data, the methane is predominantly of secondary microbial origin (Meister et al., 2018; Saroni et al., 2020).

The general bathy-morphological setting of the study area (Spatola et al., 2023) highlights several fluid-related structures (i.e., several mud volcanoes and hundreds of pockmarks), morphological highs possibly related to piercement structures, escarpments, channels and bedforms. The detailed morphological characterization of the mud volcano responsible for the 2017 outburst (named Scoglio d'Affrica MV_1, SdAMV[1]) is reported in Casalbore et al. (2020). It consists of two mounds

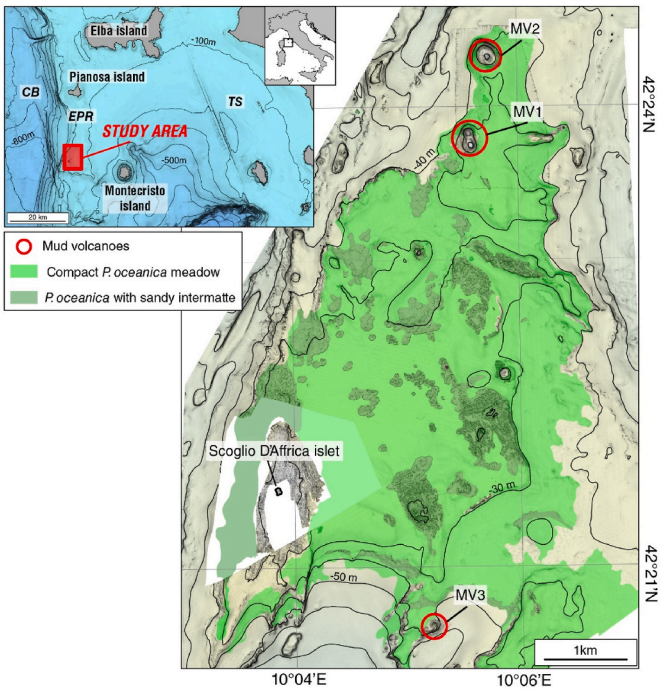

Fig. 1. Study area and bathymetric map of the Scoglio d'Affrica (contour line spacing equals 10 m). The distribution of mud volcanoes and continuous and discontinuous *P. oceanica* meadows is from Spatola et al. (2023). Bathymetry in the upper left inset is obtained from Emodnet bathymetry (https://emodnet.ec.europa.eu/); contour line spacing equals 100 m.

(M1 and M2) located at a water depth of approximately 10 m separated by a 15 m deep flat saddle. At the time of the measurements, the top of the southern mound was characterized by a smooth seafloor, covered by widespread mud breccia emitted by a 15–20 m wide ring-shaped crater, and diffuse seepage, as observed on videos collected using a Remotely Operated Vehicle (ROV). This smooth seafloor was surrounded by a blocky facies, except for the western flank where multiple mudflows were recognizable. The northern mound was dominated by a blocky facies at its top (except for small and confined smooth areas) and upper slope. The flanks of the mud volcano were generally steep (higher than 16° in the upper part) and smooth, except for the lower part characterized by a seafloor with small-scale roughness. This morpho-acoustic facies, groundtruthed by ROV observations, houses dense *Posidonia oceanica* meadows that are widespread down to −40 m depth and cover about 36% of the surveyed seafloor (Spatola et al., 2023). In some areas this facies laterally shifted to a dimpled morpho-acoustic facies, characterized by the presence of oval depressions that are a few metres to tens of metres wide and up to 2 m deep, corresponding to intermatte areas (i.e., sandy patches) that interrupt the continuity of the *P. oceanica* meadows. The interpretation of this morpho-acoustic facies agrees with previous studies, reporting dense sea grass meadows alternating with a seafloor floored by rhodoliths and bioclastic sand (Del Bono and Giammarino,1968; Fravega and Vannucci, 1982; Cinelli et al., 1993).

3. Materials and methods

3.1. Sampling strategy

Three sampling surveys were carried out during May 2021, June 2022 and July 2023 in the depth interval 8–46 m. During the first survey, 11 seafloor samples and one *P. oceanica* sample (leaves and rhizomes, P4) were collected through grab sampling. Most were located at the top (G1, G9, G10, and G13) or along the flanks (G2, G7 and G11) of mud volcanoes. Three samples were collected inside (G3, G4, G5) and at the edge (P4) of the intermatte areas within the dimple acoustic facies and one sample was retrieved from a morphological high along the western flank of the Elba-Pianosa ridge (G6) (Fig. 2, Table 1). The other two surveys were performed on the $SdAMV_1$ by scuba divers. A total of 9 seafloor samples and 3 *P. oceanica* samples were recovered at Mound1 (M1: S1-S3, P1) and Mound 2 (M2: S4-S9, P2, P3) during the 2022 survey, while 6 seafloor samples (S10-S15) were collected only at Mound 2 (M2) during the 2023 survey (Fig. 2). The main advantage of using scuba divers was the possibility to perform targeted seafloor sampling at known distances from the main emission points in order to constrain the role of gas emissions in controlling foraminiferal assemblages. Unfortunately, the resulting sampling position is less accurate with respect to the grab samples. Scuba diver sampling was focused on two morphological settings linked to different venting activity: i) muddy sediments with a stronger emission activity and the local presence of gryphons or mudflows (Fig. 3a and b); and ii) muddy seafloor with weaker emission activity (Fig. 3c and d). Samples were collected at the point of weak leakage and 5–10 m away, at the top or flanks of the mounds.

Posidonia samples were similarly collected at the point closest to the emissions (about 5 m away) and at sites not affected by emissions. Such sampling strategy was planned to highlight potential differences in foraminiferal assemblages related to venting activity as well as to different substrates (sediment and sea grass leaves) (Table 1).

3.2. Grain-size analysis

Analyses were performed on all sediment grab samples (G1-G13), except for sample G4 due to its small volume. Analyses were carried out using dry sieving for the fraction coarser than 63 μm and a laser particle sizer for the fine-grained fraction (from 0.5 to 63 μm). Samples were pretreated using hydrogen peroxide (20% solution) and distilled water to remove organic matter and salts. Samples were dried at 40 °C in a convection oven to obtain the dry weight and then the coarse fraction (gravel and sand particles >63 μm) was subsequently separated from finer silt and clay by wet sieving. The grain-size obtained for the coarse fraction was determined by dry-sieving at one-phi intervals (ASTM series), while the fine fraction was treated with 500 mL of distilled water and a 50 mL solution of sodium hexametaphosphate ($Na_6[(PO_3)_6]$) before analyzing with a laser particle sizer (Sympatec Helos LA). The descriptive statistics of grain-size distribution (mean, standard deviation, skewness, kurtosis) and sediments were classified according to the percentage of gravel, sand, silt and clay based on the Folk and Ward classification schemes (Folk and Ward, 1957).

Crystalline phases were identified using X-Ray Diffraction (XRD) on sample powder. Measurements were performed at the Department of Earth Sciences, Sapienza University of Rome (Italy) with a Brucker D500 diffractometer, using CuKα radiation (n = 1.5418 Å), operating at 40 kV and 40 mA, and at a step size of 0.0250°.

3.3. Benthic foraminifera

Two sample types were sediment and *P. oceanica* (rhizomes and leaves). Different treatments were adopted for each following, as far as possible, the standard procedures (Langer, 1993; Schönfeld et al., 2012; Mateu et al., 2014).

Sediment (the upper 2 cm layer of the grab and scuba samples) was collected for benthic foraminifera analysis and stored in plastic containers. To distinguish the living fauna, all sediment samples were stained and preserved in a solution of 90% ethanol with 2 g/L of Rose Bengal (Walton, 1952; Lutze and Altenbach, 1991; Schönfeld et al., 2012). After 15 days, the samples were wet sieved through a 63 μm sieve and then dried at 40 °C. For each sample, living (stained) and dead foraminifera were counted, hand-picked, and identified using a binocular stereomicroscope. To detect living porcelaneous specimens, each test was broken. The Rose Bengal staining method has been widely used

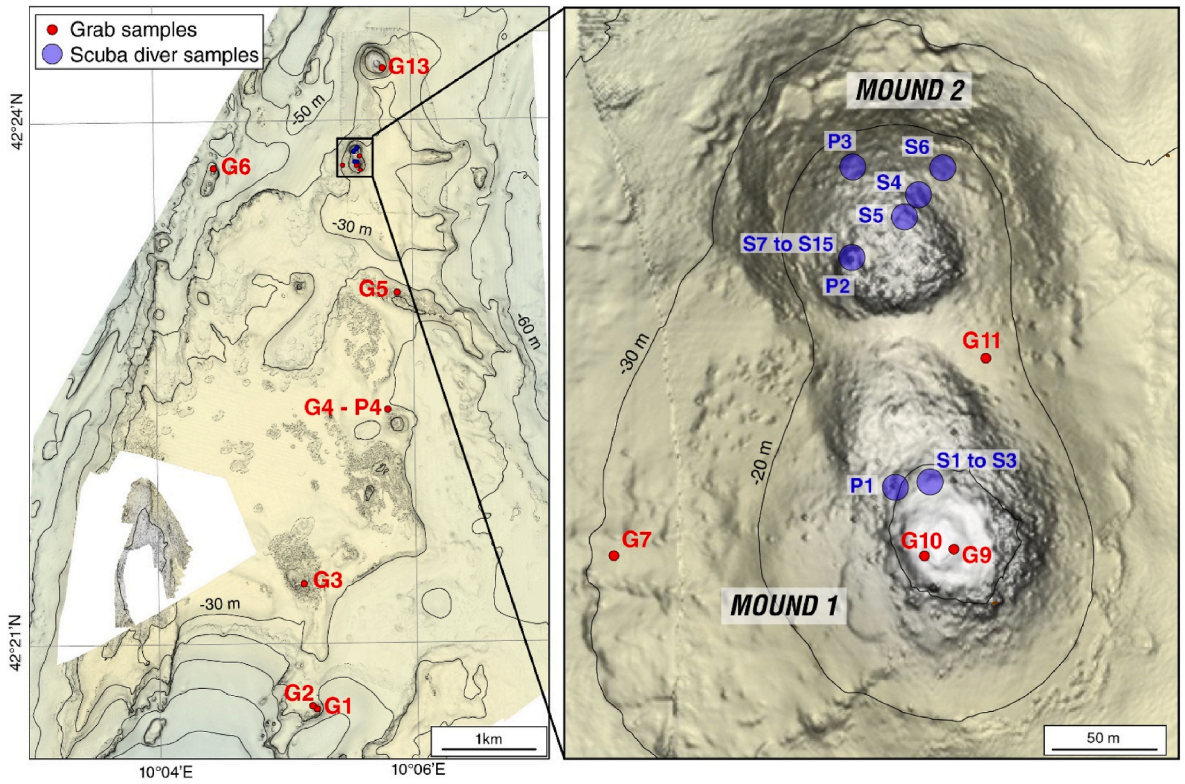

Fig. 2. Location of the sampled sites. The red dots denote the position of the grab samples collected in 2021, while the blue circles indicate the approximate areas where scuba divers collected sediment and *P. oceanica* samples in 2022 and 2023 on Mounds 1 and 2.

Table 1
Summary of sampling stations: grab and scuba sample ID, coordinates, depth and sample location EPR*: Elba- Pianosa Ridge.

Grab Sample ID	Lat	Long	Depth	Location
G1	42°20′37"N	10°05′13"E	28m	Top MV3
G2	42°20′38"N	10°05′11"E	33m	Flank of MV3
G3	42°21′20"N	10°05′08"E	21m	Intermatte zone
G4	42°22′20"N	10°05′47"E	28m	Intermatte zone
G5	42°23′00"N	10°05′53"E	25m	Intermatte zone
G6	42°23′44"N	10°04′28"E	46m	Flank of EPR* morphological high
G7	42°23′44"N	10°05′28"E	29m	Flank of MV1(mud flow)
G9	42°23′44"N	10°05′34"E	8m	Top M1 (edge of the new crater) of MV1
G10	42°23′45"N	10°05′35"E	9m	Top M1 of MV1
G11	42°23′48"N	10°05′36"E	18m	Flank M2 of MV1
G13	42°24′17"N	10°05′46"E	17m	Flank of MV2
P4	42°22′20"N	10°05′47"E	28m	Edge Intermatte zone
Scuba Sample ID	**Station area coordinates Lat**	**Long**	**Depth**	**Location**
S1-S3	42°23′45"N	10°05′35"E	8m	Top M1 of MV1
S4	42°23′50"N	10°05′35"E	13m	Top M2 of MV1
S5	42°23′50"N	10°05′34"E	11m	Top M2 of MV1
S6	42°23′51"N	10°05′35"E	16m	Flank M2 of MV1
S7-S15	42°23′49"N	10°05′33"E	10m	Top M2 of MV1
P1	42°23′45"N	10°05′34"E	10m	Top M1 of MV1
P2	42°23′49"N	10°05′33"E	10m	Top M2 of MV1
P3	42°23′51"N	10°05′33"E	15m	Flank M2 of MV1

in ecological studies to distinguish living from dead foraminifera because it is inexpensive and easy to use (Bernhard, 2000; Scott et al., 2001; Murray, 2006). However, under specific conditions (i.e., anoxic environments) the accuracy of this method may be affected by the presence of undecayed protoplasm, which can persist for weeks or months after death (Bernhard, 1988, 2000; Hannah and Rogerson, 1997;

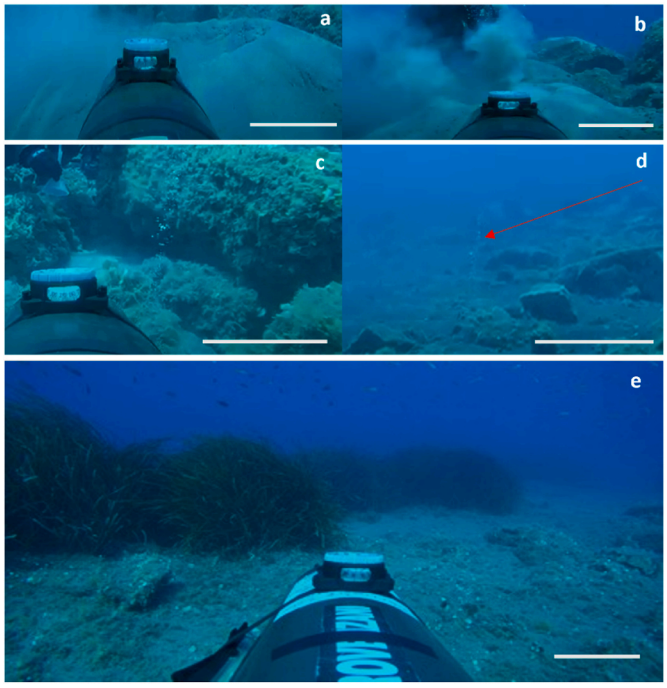

Fig. 3. a-b) Gryphons associated with a stronger emission activity (MV1); c-d); weak emissions (marked by a red arrow, MV1); e) *Posidonia* meadow along the flank of MV1. The white bar indicates an approximate reference scale of 20 cm. Photos by BigBlueXplorers.

Murray and Bowser, 2000). While the staining criteria are confidently applied to the superficial samples, ambiguities may arise in the case of deeper intervals (Fontanier et al., 2002), commonly consisting of a slight

overestimation of the living assemblages (Frontalini et al., 2018). In spite of this, the Rose Bengal method, when used with care, yields results that are as reliable as those obtained using other techniques (Lutze and Altenbach, 1991; Murray and Bowser, 2000; Figueira et al., 2012). The quantitative analysis of benthic foraminifera was based on the count of all specimens present in the whole sample. For the count of dead specimens, in order to prevent the inclusion of reworked or transported tests, only well-preserved tests that were not re-crystallized and were free of cracks and abrasions, were picked, counted and identified. The absolute abundance of living and dead foraminifera was calculated as the foraminiferal number (FN), defined as the number of specimens per gram of dry sediment (Schott, 1935). The species diversity, given by the H-index (Shannon, 1948) and as total number of taxa in the sediments (S), was calculated using the statistical package Palaeontological Statistics-PAST 4.13 (Hammer et al., 2001; Hammer and Harper, 2006).

P. oceanica samples –Two rhizomes and 3 to 4 leaves with similar lengths were analyzed for each site, resulting in a total of 10 rhizomes and 20 leaves. *P. oceanica* rhizomes were cut off from the substrate approximately 1 cm above the sediment surface. Leaves and rhizomes were immediately stowed in water-filled plastic bags and later carefully washed with seawater over a 63 μm sieve. Epiphytes were washed into larger bowls, washed with fresh water and dried. Plant fragments were examined under the microscope to remove living specimens that may have remained glued to the plant surface. All epiphytic foraminifera were picked from each sample and identified at the species level. The ratio between number of specimens recorded and number of leaves analyzed (F/P) was calculated to have a broad estimation of epifaunal density (Di Bella et al., 2022).

Genus-level classification was made according to the most used taxonomical study on foraminiferal genera (Loeblich and Tappan, 1987), while species were determined according to some important studies conducted in the Mediterranean area (Cimerman and Langer, 1991; Sgarrella and Moncharmont-Zei, 1993; Panieri et al., 2005) as well as the World Modern Foraminifera Database (Hayward et al., 2011). Some species were grouped for a better and more direct understanding of foraminiferal distribution patterns: rosalinids include *Neoconorbina* spp., *Gavelinopsis praegeri*, *Rosalina* spp. (see appendix) (Cimerman and Langer, 1991; Langer, 1993) muddy preference foraminifera include some Low Oxygen Foraminiferal Assemblages (Bernard and Sen Gupta, 1999) like *Bolivina* spp., *Bulimina* spp., *Fursenkoina acuta*, *Cassidulina* spp.; and the cibicids group includes *Cibicides refulgens* and *Lobatula lobatula* (Langer, 1993). The foraminiferal content was also analyzed on the agglutinated, porcelaneous and hyaline test. The quantitative data of the three tests were considered because the biomineralization can change as response to the physical and chemical seafloor conditions (Pettit et al., 2013; Di Bella et al., 2022; Yanko et al., 2023). To investigate the morphological, structural, and compositional characteristics of tests, Scanning Electron Microscope SEM, FEI Quanta 400, and Energy Dispersive X Ray Spectroscopy EDS measurements were made at the SEM Laboratory of the Earth Sciences Department, Sapienza University of Rome. A similar qualitative approach was used to examine the carbonate crusts that were found in most of the sediment samples.

The samples were attached to 12.5 mm SEM stubs using carbon tabs and then coated with a conductive layer (5–15 nm) of gold (Au) using an Emitech K550X sputter coater and a routine cycle time of typically less than 4 min. Samples were viewed in high vacuum mode using an accelerating voltage of 20 kV; the focus was adjusted to match the change in working distance (~11 mm) over the same range of the specimen and an improved image was obtained, ranging between 5 and 300 μm resolution.

3.4. Isotopic analyses

Three samples of *P. oceanica* (leaves), belonging to both near emissions and background sites, were analyzed for stable carbon isotope ratios and then compared with a sample belonging to the *P. oceanica* meadows of Maratea (southern Italy), here used as a reference for an undisturbed, healthy environment.

To eliminate all the carbonate fraction belonging to the epiphytic organisms, the *Posidonia* samples were dipped in an 18% HCl solution for 10 s, abundantly rinsed with distilled water to stop the reaction and remove any trace of acid, and then dried at 40 °C.

Organic carbon isotope ratios ($\delta^{13}C_{TOC}$) were measured with a Finnigan Delta V Advantage Mass spectrometer coupled with a Flash 2000 Thermo Elemental Analyzer at the stable isotope laboratory of the Earth Sciences Department of Sapienza University of Rome. All the results were calibrated against the international standard Wheat Flour OAS. Analytical error is ±0.2‰ based on replicate standard analyses run together with the samples (N = 14).

3.5. Gas

Three gas samples were collected at different locations on the top of M2 on 18/07/2023. Bubbles were captured using an inverted funnel connected to a 1L glass ampule with inlet and outlet stopcocks and a gas sampling port. The funnel was held in place by a diver at a height of about 20 cm above the sea floor until the collected gas had displaced all seawater in the ampule. The samples were stored at room temperature and analyzed within 2 weeks using a Carlo Erba 8000 model gas chromatograph with helium carrier gas. Light hydrocarbons (C1 to C4) were separated on a 2m long CBK-BHT100 packed column and analyzed using a Flame Ionization Detector while carbon dioxide was separated on a 2m long Porapak-Q packed column and analyzed using a Thermal Conductivity Detector. Analytical reproducibility (1σ) is about ±5%.

4. Results

4.1. Sediment characteristics

Two main types of sediments can be distinguished. The first group mainly consists of bioclastic sand and gravel recovered from intermatte areas on discontinuous *P. oceanica* meadows and on a morphological high in the western sector of the study area. The second group mainly consists of silty sediment with a variable proportion of gravel and cobbles, sampled at the top of the mud volcanoes or along their flanks (Fig. 4).

Sediments with a dominant bioclastic component (G3, G5, G6) consist of poorly to moderate sorted gravelly sands or sandy gravel, with a gravel content ranging between 19 and 47% and a silty/clayey content of <4% (Table 2). The inorganic sandy fraction is constituted mainly by quartz. The bioclastic fraction is characterized by fragmented and intact mollusks (bivalves and gastropods), bryozoans, serpulids, diatoms, echinoids, ostracods and foraminifera.

Sediments with fine- and coarse-grained fraction include heterogeneous sediment classes that range from gravelly mud to slightly gravelly sandy mud, all showing very poor sorting and coarse skewness, except for samples G1 (characterized by fine skewness) and G2 (with a symmetric distribution). The gravel and sand contents range from 1.4 to 13.2% and from 15 to 50%, respectively, while the fine-grained fraction (i.e. silt and clay) is between 45 and 80%. On the basis of diffractometer analyses, the coarser fragments are primarily carbonates (Mg-calcite and, to a lesser extent, Fe-(Mn)-bearing dolomite (ankerite), Fig. 5a). Carbonate gravels are held together by the fine-grained fraction, formed by prevailing clay minerals (kaolinite, montmorillonite, illite) and phyllosilicates (muscovite, chlorite) plus subordinate quartz (Fig. 5b).

SEM-EDS analyses show that some carbonate fragments have a concave crust morphology (Fig. 6A), which locally has an ankerite composition (Fig. 5A), while the matrix has a clay composition (Figs. 5B and 6B). The faunal content, which is very scarce, is represented by few specimens of bivalves and foraminifera. No bioclastic fraction is present.

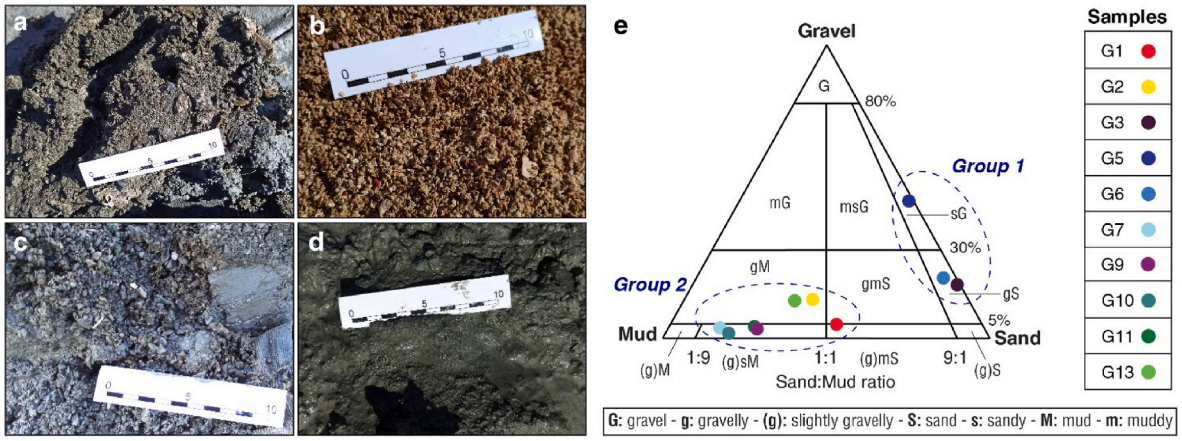

Fig. 4. Main types of sediment samples: a) G2: gravelly mud; b) G3: bioclastic gravelly sand; c) G7: slightly gravelly sandy mud (with higher gravel content); and d) G10: slightly gravelly sandy mud. e) Ternary diagram for the grab samples collected in 2021, showing the two main sediment types occurring in the study area. Sediment classification scheme from Folk and Ward (1957).

Table 2
Granulometric characteristics of sediment grab samples in the study area. (Slgr = slightly gravelly).

Sample	% Gravel	% Sand	% Silt	% Clay	Mean (phi)	Sorting	Skeweness	Kurtosis	Folk Class
G1	4.96	49.79	25.17	20.08	4.43	3.31	0.25	0.76	(Slgr) Muddy sand
G2	13.19	39.46	24.15	23.2	3.95	4.08	0.06	0.78	Gravelly mud
G3	18.56	81.03	0.33	0.08	−0.55	0.58	−0.03	1.21	Gravelly sand
G5	47.72	51.74	0.44	0.1	−1.05	0.79	−0.16	1.08	Sandy Gravel
G6	20.89	75.93	1.94	1.24	0.23	1.53	0.13	1.03	Gravelly sand
G7	3.54	15.83	38.69	41.94	6.43	3.21	−0.59	1.53	(Slgr) Sandy mud
G9	3.99	27.19	37.3	31.52	5.83	3.34	−0.42	0.76	(Slgr) Sandy mud
G10	1.37	19.37	40.3	38.96	6.5	2.86	−0.49	1.05	(Slgr) Sandy mud
G11	4.02	26.35	40.42	29.21	5.81	3.25	−0.38	0.82	(Slgr) Sandy mud
G13	12.84	33.82	29.19	24.15	4.42	4.11	−0.27	0.69	Gravelly mud

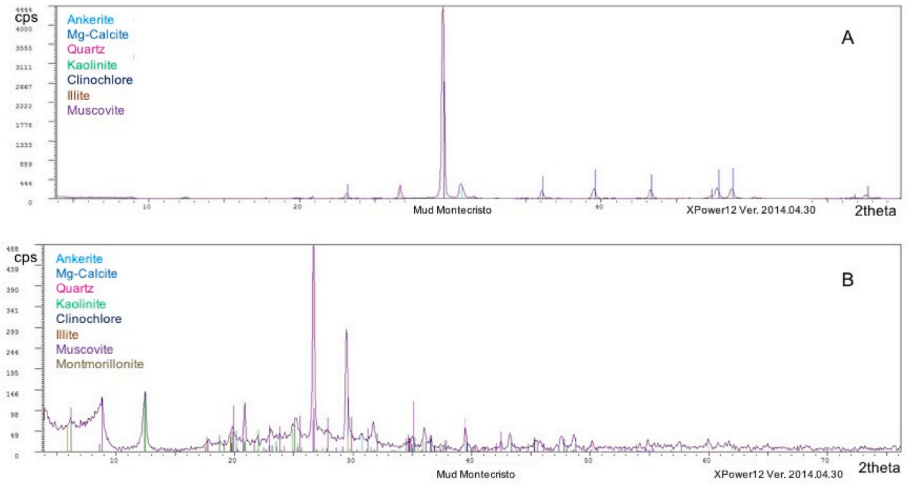

Fig. 5. X-ray diffraction pattern of a sample representative of the mineral assemblage constituting the carbonate clasts (A) and the muddy sediments (B).

4.2. Gas composition

Based on qualitative observations by the divers, bubble emission rates were significantly lower during the 2023 campaign when these samples were collected compared to that conducted in 2022. All gas bubble samples have a very similar composition (Table 3) that consists of about 95% methane, 350 ppm ethane, 4 ppm propane, 1% CO_2 and a $CH_4/(C_2H_6+C_3H_8)$ ratio of about 3000. These values are very similar to those reported by Saroni et al. (2020) for samples collected in 2018 from bubble emissions in the same area. Gas flux rates, at standard temperature and pressure conditions, are reported for two of the three points.

4.3. $\delta^{13}C_{TOC}$ analyses

The $\delta^{13}C_{TOC}$ of *P. oceanica* leaves in the Scoglio d'Affrica area ranges between −15.48‰ and −18.30‰, with the heaviest value recorded at a non-emission site (P3) and the lightest one at an emission site (P2). Conversely, the Maratea sample shows the heaviest C isotope signature of −13.63‰ (Table 4).

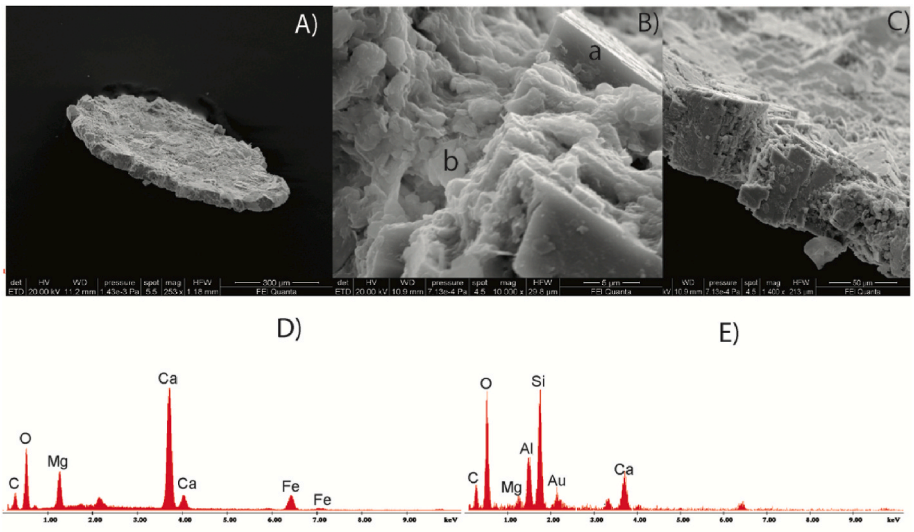

Fig. 6. SEM images of a carbonate crust (A); detail of carbonate crust (B): a) carbonate crystals and b) silicate matrix. C) Detail of the thickness of the crust; diatoms are visible. The related EDS spectra of a) and b) are given in D) and E), respectively.

Table 3
Gas concentrations of sampled bubbles. Note that gas flux rates are at Standard Temperature Pressure (STP) conditions. n/a – not analyzed.

Sample ID	CH_4 (vol%)	C_2H_6 (ppm)	C_3H_8 (ppm)	CO_2 (vol %)	C1/ (C2+C3)	Gas flux (ml/min)
B1	94.8	375	4.2	0.8	2500	200
B2	94.5	285	3.8	0.8	3272	30
C	92.8	350	3.9	1.1	2622	n/a

Table 4
Summary of $\delta^{13}C_{TOC}$ values of *P. oceanica* leaves from the study area (P1-P3 samples) and from a site not influenced by venting activity (MAR samples).

Sample ID	δ13C	Dev.St.P	δ13C mean
MAR	−13.68		
MAR	−13.57	0.06	−13.63
P1	−17.04		
P1	−16.81	0.12	−16.93
P3	−15.51		
P3	−15.45	0.03	−15.48
P2	−18.43		
P2	−18.17	0.13	−18.30

4.4. Living and dead foraminiferal assemblages

Sediment samples - The foraminiferal content (living and dead assemblages) is widely variable across the study area (Fig. 7). Ten samples are totally barren (G1, G7, G10, G11, S1, S4, S5, S7, S14 and S15). In most samples the dead assemblage clearly prevails over the living one, except for G9 (M1), S8, S12 and S13 (M2) where the living specimens were dominant.

The dead assemblage includes a total of 109 species (Appendix). Agglutinated taxa are scarcely represented, being absent or with abundances <6% in most samples. In contrast, both the porcelaneous group and hyaline taxa are abundant, with values ranging from 15.91 to 79.46% and from 20.54 to 78.41%, respectively (Table 5).

The living (stained) assemblage includes a total of 84 species (Appendix). The agglutinated taxa are more frequent and diversified with respect to the dead assemblage, although they are totally absent in G6 and S2. The porcelaneous taxa are abundant with percentages ranging from 8.93 to 66.67%, except in sample G3 where they are not found. Hyaline taxa are dominant in all samples, similarly to the dead assemblage, with percentages ranging from 33.33 to 84.62% (Table 6).

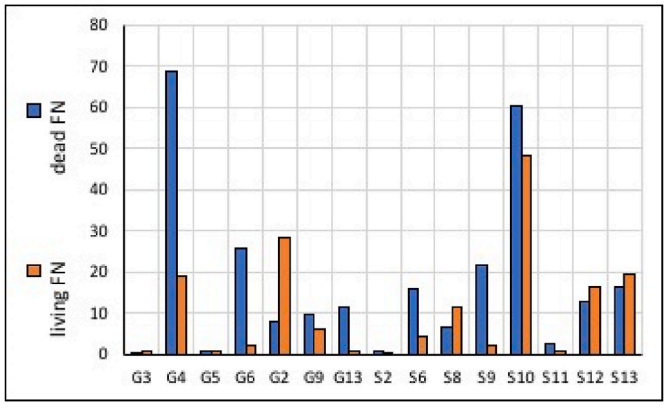

Fig. 7. Comparison of the density (FN = vertical axe) of living and dead benthic foraminifera in each sample.

Posidonia oceanica samples - *P. oceanica* leaves and rhizomes are characterized by the presence of encrusted organisms like serpulids, corallinaceous algae, bryozoans and diatoms. The foraminiferal content consists of a total of 1233 individuals on all leaves and rhizomes. The diversity is higher on the leaves (mean value H = 2.49) than on the rhizomes (mean value H = 1.43). The highest density value for both rhizome and leaf samples was recorded in sample P4 (327.43 F/P), collected at the edge of an intermatte zone in the central sector of the study area, followed by sample P2 from the top of MV1-M2 (309.4 F/P) (Table 7). Although these values are similar, it should be noted that the foraminiferal content is mainly concentrated on the leaves in P2 (emission zone) and on the rhizomes in P4. The lowest F/P value is recorded in sample P3 near the top of MV1-M2 (99.71 F/P). Agglutinated taxa are very few or totally absent, both in the rhizomes and leaves, while porcelaneous species seem to mainly prefer the rhizome microhabitat. The hyaline specimens dominate both on leaves and rhizomes (Table 7, Fig. 8).

The list of observed species is reported in Appendix. Some species, like *Cibicidella variabilis*, *Peneroplis* spp., *Miniacina miniacea*, the most part of Miliolids and the agglutinated taxa, are recorded exclusively in the rhizomes. Rosalinids (*Neoconorbina posidonicola*, *Gavelinopsis praegeri*, *Rosalina* spp.) are dominant both on the leaves and rhizomes, with

Table 5
Foraminiferal density (FN) and percentages of Agglutinated, Porcelaneous and Hyaline taxa, total number of individuals (N), number of taxa (S), diversity index (H) of dead assemblages calculated for each sample in which foraminiferal content was recorded. Barren samples are not reported.

Samples	FN ind/g	Agglutinated %	Porcelaneous %	Hyaline %	N	S	Shannon_H
G3	0.26	0.00	30	70	10	6	1.61
G4	68.79	1.48	20.2	78.33	205	34	2.72
G5	0.53	0.00	33.33	66.67	18	9	1.98
G6	25.70	4.00	27.43	68.57	175	38	3.19
G2	7.71	0.51	33.33	66.16	198	37	3.20
G9	9.69	5.68	15.91	78.41	88	36	3.27
G13	11.53	1.36	53.39	45,25	221	48	3.43
S2	0.66	0.00	62.5	37.5	48	17	2.38
S6	15.98	0.00	58.62	41.38	58	26	3.10
S8	6.27	0.00	66.67	33.33	75	29	3.00
S9	21.80	0.00	47.83	52.17	23	14	2.53
S10	60.19	0.00	78.65	21.35	192	41	3.41
S11	2.36	0.00	71.88	28.13	64	19	2.62
S12	12.79	1.40	61.54	37.06	143	40	3.25
S13	16.30	0.00	79.46	20.54	112	26	2.84

Table 6
Foraminiferal density (FN) and percentages of Agglutinated, Porcelaneous and Hyaline taxa, total number of individuals (N), number of taxa (S), diversity indices (H) of living (stained) assemblage calculated for each sample.

Samples	FN ind/g	Agglutinated %	Porcelaneous %	Hyaline %	N	S	Shannon_H
G3	0.90	60.00	0.00	40.00	30	6	1.47
G4	19.13	23.21	8.93	67.86	56	23	2.71
G5	0.50	33.33	13.33	53.34	15	10	2.12
G6	1.90	0.00	15.38	84.62	13	8	1.83
G9	28.41	5.43	38.75	55.82	258	46	3.22
G2	6.07	20.13	18.18	61.69	154	33	3.04
G13	0.73	10.00	50.00	40.00	10	6	1.70
S2	0.19	0.00	42.86	57.14	14	8	1.97
S6	4.13	6.66	26.67	66.67	15	9	2.06
S8	11.34	0.00	66.67	33.33	39	11	1.67
S9	1.91	14.28	42.86	42.86	7	6	1.75
S10	48.27	4.55	19.48	75.96	154	22	2.27
S11	0.63	1.39	36.11	62.50	72	20	2.61
S12	16.19	2.76	37.02	60.22	181	31	2.82
S13	19.21	0.76	30.30	68.94	132	24	2.53

the highest percentages at MV1 (M1 and M2).

Regarding the state of preservation, it should be highlighted that tests collected in the methane emission were poorly preserved. In fact, the SEM analyses highlight strong signs of cracks and fractures, resulting in increased shell fragility in all *P. oceanica* samples and leading to the formation of calcined shells (mainly in the miliolids and rosalinids tests) in the sediment samples. Moreover, in many cases the foraminifera are very small and have morphological alterations. Calcite crystals are also present in the samples collected near the emissions (Fig. 9).

4.4.1. Distribution of dead and living foraminiferal assemblages

The areal distribution of foraminiferal assemblages is described below according to the characteristics of the different sampling locations, which can be grouped into four main settings.

(i) *Areas with strong emission activity, locally associated with gryphons and mud flows* –Samples collected in these areas (G1, G10, S1, S3 to S5, S7, S14 and S15) were totally barren of foraminiferal content. They were collected at or very close to the strongest emissions at the top of MV1 and MV3.

(ii) *Mud flows along the flanks of MV1* – Similar to the previous samples, these (G7, G11) also lack microfauna, although no specific point emissions were detected at the time of sampling.

(iii) Muddy sediments associated with weak emissions– Samples (S2, S6, S8-13, G2, G9, G13, P1, P2, P3) range from 0.19 to 48.27 ind/g for the living assemblage and 0.66 to 60.19 ind/g for the dead one (Tables 5 and 6). The living specimens are only dominant in the samples collected at MV1 (M1: G9 and M2: S8, S12, S13). In the dead assemblage, the agglutinated taxa are absent in most samples. The highest percentage (5.68%) is recorded in sample G9. The presence of Eggerolloides advenus, Lepidodeuterrammina ochracea, Reophax sp. and Textularia spp. is scarce. The porcelaneous group is abundant, with percentages ranging from 15.91 to 79.46%. In most MV1 samples, these taxa are >40%. The most common species are miliolids (Adelosina spp., Quinqueloculina spp., Triloculina spp.) and Peneroplis spp. (Appendix). Hyaline taxa range from 21.35 to 78.41%, with values > 30% in all samples except for S10, S11 and S13 (MV1) (Table 5). The most common are rosalinids and cibicids, which are associated with other typical shallow water taxa like Buccella frigida, Elphidium and Glabratella spp. (Appendix). The diversity index (H) values are always >2, ranging from 2.38 to 3.43.

For the living assemblage, the agglutinated taxa represent 20.13% and 14.28% in G2 and S9, respectively, but are absent or scarcely represented in the other samples. The porcelaneous group is frequent, ranging from 18.18% to 66.67% in most samples. *Quinqueloculina stelligera* is the most abundant species (mean value 9.07%) with the maximum abundance recorded in samples G13, S8 and S9 (Fig. 10). However, at the top of M1 (MV1: G9), high frequencies of *Affinetrina gualtieriana*, *Siphonaperta aspera*, *Quinqueloculina bosciana* and *C. involvens* are recorded. Hyaline taxa are dominant in all samples, similar to that recorded in the dead assemblage, with percentages ranging from 33.33% to 68.94%. Overall, the living assemblage reflects the composition of the dead one. Rosalinids and miliolids represent the most abundant taxa, with mean percentages of 27.52% and 24.20%,